Available online at www.sciencedirect.com
SCIENCE DIRECT
Thin Solid Films 496 (2006) 412 – 416
thin solid films
www.elsevier.com/locate/tsf

Kinetics of cuprous oxide etching with β-diketones in Supercritical CO_2

Xiaoying Shan, James J. Watkins *

Department of Chemical Engineering, University of Massachusetts Amherst, MA, 01003, USA

Received 10 January 2005; received in revised form 12 July 2005; accepted 16 August 2005
Available online 3 October 2005

Abstract

Cuprous oxide films (Cu_2O) supported on Cu or on SiO_2 were etched using solutions of β-diketones including 1,1,1,5,5,5-hexafluoroacetylacetone, 2,2,6,6-tetramethyl-3,5-heptanedione and 2,2,7-trimethyl-3,5-octanedione (TMOD) in supercritical carbon dioxide at temperatures between 80 and 150 °C and pressures between 20 and 27.5 MPa. The films and etched substrates were analyzed by X-ray photoelectron spectroscopy depth profiling, field emission scanning electron microscopy and spectroscopic ellipsometry. Each of the etching agents was effective. Etching kinetics using TMOD were measured at 100, 125 and 150 °C. At 150 °C the etch rate was 1.5 nm/min. Based on the activation energy obtained from the studies (66 kJ/mol), etching rates of greater than 10.0 nm/min can be obtained at 200 °C.
© 2005 Elsevier B.V. All rights reserved.

PACS: 82.20.Pm; 82.80.Pv
Keywords: Etching; Cuprous oxide; Supercritical fluid

1. Introduction

Copper has replaced aluminum as the interconnect material of choice in advanced integrated circuits. While copper offers lower resistivity (1.7 μΩ cm) and superior electromigration resistance, it is more difficult to integrate than Al. Cu is easily oxidized and the native oxide layer of copper, unlike that of Al, does not self-passivate. The presence of copper oxides at film interfaces in interconnect structures is problematic for a number of reasons including increased resistivities, poor adhesion and greater susceptibility to electromigration [1,2].

Several approaches have been proposed to prevent or remediate Cu oxidation during device fabrication. Cu surfaces can be passivated by implantation of dopants or by the formation of alloys, silicides or nitrides [3]. Another option is to minimize exposure of Cu to oxidizing atmospheres and to remove any copper oxides generated through adventitious oxidation in situ via etching. For example dry etching processes remove Cu oxides by vapor phase exposure to volatile etchants including 1,1,1,5,5,5-hexafluoroacetylacetone (Hhfac) at elevated temperatures [4,5]. Cu oxide etching by Hhfac is proposed to proceed via:

$$CuO(s) + 2Hhfac(g) \rightarrow Cu(hfac)_2(g) + H_2O(g) \quad (1)$$

$$Cu_2O(s) + 2Hhfac(g) \rightarrow Cu(hfac)_2(g) + Cu + H_2O(g). \quad (2)$$

This mechanism suggests that Cu metal is not etched directly by Hhfac. Rather Cu films can be etched by simultaneous or sequential exposure to the etching agent and an oxidizer such as H_2O_2 or an O_2 plasma [6–9]. Typically high temperatures (>500 K) are required for acceptable etching rates [4]. Moreover, high volatility of the etching agents and the resulting metal chelate byproducts are prerequisites for efficient dry etch processes. To promote volatility, fluorinated compounds such as Hhfac are typically used as the etching agent. However, in addition to undesirable environmental impact, the use of these species can lead to fluorine contamination at the interface, which has a deleterious impact on performance issues including adhesion [10].

Supercritical fluids (SCFs) including carbon dioxide offer an alternative medium for dry etch chemistry. Their advantages lie in their physicochemical properties. The densities of SCFs, including carbon dioxide, can approach or exceed that of liquids, enabling the dissolution of reagents and byproducts. However, the transport properties of SCFs, including low

* Corresponding author. Tel.: +1 413 545 2569; fax: +1 413 545 1647.
E-mail address: watkins@ecs.umass.edu (J.J. Watkins).

0040-6090/$ - see front matter © 2005 Elsevier B.V. All rights reserved.
doi:10.1016/j.tsf.2005.08.274

viscosity, high diffusivity and the absence of surface tension are closer to those of a gas. For dry etch chemistry, the implications are clear. Transport of the etching agent and metal chelate byproducts in solution obviates species volatility requirements, eliminates the need for fluorinated reagents, and potentially mitigates mass transfer resistance during etching. These benefits are realized while maintaining many of the advantages of a vapor phase process. Moreover, SCF-based etching is compatible with other emerging processes for semiconductor devices that employ supercritical fluids. Recently we and others have demonstrated the utility of SCFs for the deposition of metals [11–18] and dielectic films [19] for device applications. Much effort has also been directed towards cleaning and photoresist stripping in SCFs [20].

DeSimone et al. recently demonstrated etching of Cu metal films in carbon dioxide using solutions of ethyl peroxydicarbonate as the oxidant and various diketones as the etching agent [21]. Etching rates were not measured. Here we report the direct etching of Cu_2O from the surface of Cu and SiO_2 using solutions of Hhfac, 2,2,6,6-tetramethyl-3,5-heptanedione (TMHD) and 2,2,2-trimethyl-3,5-octanedione (TMOD) in supercritical CO_2 and present kinetic data for oxide etching using TMOD at 100, 125 and 150 °C. We also note the impact of a surface layer containing Cu^{2+}species on etching efficiency.

2. Experimental details

Hhfac and TMHD were purchased from Sigma-Aldrich (St Louis, MO). TMOD was purchased from Epichem Inc. (Allentown, PA). The structures of the etching agents are shown in Fig. 1. All were used as received.

Two copper oxide test structures (donated by Novellus Systems Inc.) were used in the experiments (Fig. 2). The “type A” wafer was comprised of a $Cu_2O/Cu/SiO_2/Si$ film stack. The thickness of the cuprous oxide layer was 14.0–15.5 nm, while the underlying Cu layer was about 200 nm thick. The “type B” test stack had a multilayer structure comprised of $Cu_2O/SiO_2/Si$. The thickness of the Cu_2O layer was ~80 nm as determined by scanning electron microscopy (SEM, JEOL 6320F) operating at 5 kV and variable angle spectroscopic ellipsometry (VASE, SOPRA GES-5). The VASE data was analyzed and modeled with a multilayer stack structure using the software WINELLI (version 4.07) provided by SOPRA.

The etching experiments were conducted in a 20 ml 316 stainless steel batch reactor heated using a resistance heating tape regulated with a proportional, integral and derivative controller (Fig. 3). Temperature was measured within the vessel using a thermocouple. In a typical experiment, the test structure was loaded into the reactor within a N_2-purged glove box, the reactor was sealed, removed from the glove box and purged with CO_2 at 60 °C and 7.0 MPa using a high pressure syringe pump (ISCO Inc.). The reactor was heated to the desired temperature and the outlet valve was closed. The etching agent was then introduced to the reactor by directing CO_2 flow from the ISCO pump through a 6-port high performance liquid chromatography (HPLC) sample loop

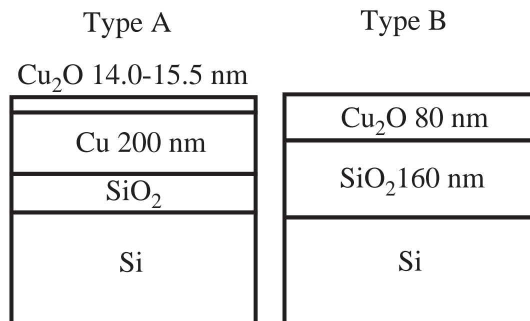

Fig. 2. Structures of the test stacks used in the experiments.

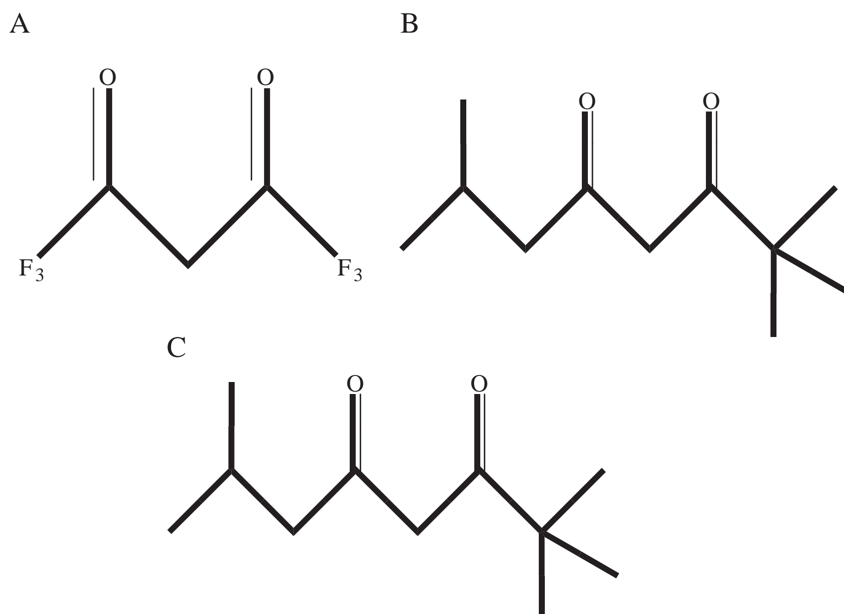

Fig. 1. Etching agents used in this study A) Hhfac; B) TMHD; C) TMOD.

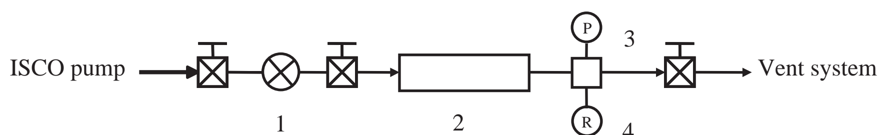

Fig. 3. Schematic of the etching system. 1. 6-port HPLC sample injector; 2. batch reactor; 3. pressure gauge; 4. safety head and rupture disk.

loaded with 0.2 ml of the etching agent upstream of the reaction vessel. CO_2 flow through the sample loop was maintained until the desired reactor pressure was achieved. After etching for a known period of time, the reactor was vented and the effluent was directed through an activated carbon bed and a bubbler within a fume hood. The reactor was then flushed with pure CO_2 at 60 °C and 7.0 MPa prior to opening. Coleman grade CO_2 was used for feasibility experiments and supercritical fluid extraction grade CO_2 (Brin's Oxygen Company Limited, 99.9999%) was used for the kinetic experiments.

The wafers were analyzed by X-ray photoelectron spectroscopy (XPS). For the kinetic measurements a Quantum 2000 scanning ESCA Microprobe (PHI) equipped with an Ar^+ion-sputtering gun located at the University of Massachusetts was used. Composition vs. depth profiles were generated by alternating Ar^+sputtering with XPS analysis. The take off angle for the analysis was 45° and monochromatized Al Kα 1486.6 eV X-rays were used. The XPS data were analyzed using Multipak Software provided by PHI (version 7.0). For the kinetic experiments on "Type B" wafers, Ar^+sputter rates for Cu_2O were calibrated using the known thickness of the oxide layer (80 nm). The setting for the ion gun was 3 keV and raster size of 2 by 2 mm. The current of the ions was 740 nA. All the multiplex spectra were taken with pass energy of 29.35 eV. Under these conditions, 20 min was required to sputter through the 80 nm thick oxide layer, yielding a sputtering rate of 4 nm/min. For feasibility experiments, using "Type A" wafers, XPS analysis was conducted offsite using a PHI ESCA 5800. Sputtering rates for Cu_2O were not calibrated on this instrument. Rather, sputtering times at identical ion gun settings were compared directly.

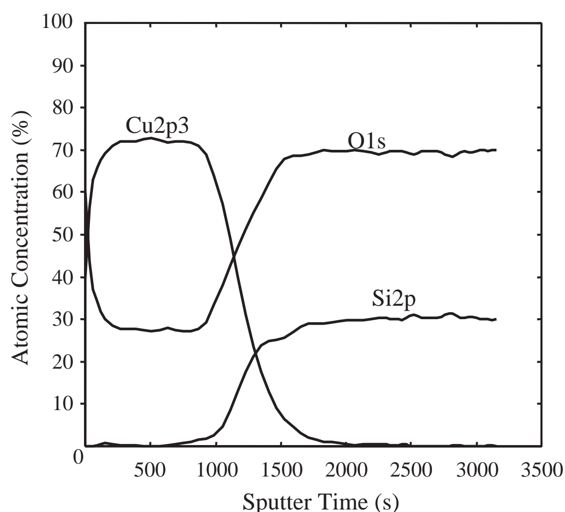

Fig. 4. XPS-depth profile of the "type B" test stack prior to etching. The thickness of the cuprous oxide layer is 80 nm. The setting of the Ar^+ion gun was 3 keV, raster size of 2 by 2 mm, 740 nA. The sputtering and analysis interval was 30 s.

3. Results and discussion

3.1. Feasibility studies

The feasibility of Cu_2O etching with β-diketones in supercritical CO_2 was assessed using "Type A" test structures and TMHD and Hhfac as etching agents. First, a control experiment was conducted in which a section of the test wafer was exposed to Coleman grade CO_2 at 150 °C and 27.5 MPa for two hours. After exposure, XPS depth profiling was conducted on both the exposed and unexposed test stacks. No significant difference in the Ar^+sputtering time required to detect 95% Cu at the wafer surface (~28 min) was observed between the wafers, indicating the thickness at the Cu_2O layer (~15 nm) did not change appreciably.

After exposure of the test stack to solutions of Hhfac (0.063 g/g CO_2) at 27.5 MPa and 150 °C for 5 min or TMHD (0.013 g/g CO_2) at 27.5 MPa and 80 °C for four hours, the Ar^+sputtering time required during XPS analysis to achieve 95% Cu at the wafer surface was reduced to 6–8 min. Clean Cu surfaces are subject to ambient oxidation and thus the short Ar^+sputtering times required to detect 95% Cu for the etched samples is not unexpected. While the etching times were chosen arbitrarily, it is evident from the data that either treatment is effective for Cu_2O etching. The XPS data also revealed that the presence of 2.1% fluorine at the film surface after Hhfac etching, indicating that the use of a fluorinated etching agents such as Hhfac can result in undesirable contamination. Given the rapid etching observed at high temperatures and the need for better resolution, test stacks containing thicker Cu_2O films were required to collect meaningful kinetic data. Consequently no further testing using the "Type A" wafers was conducted.

3.2. Kinetic experiments

TMOD was selected as the etching agent for the kinetic measurements. TMOD is non-fluorinated and similar in structure to TMHD used in the feasibility experiments. However, the solubility of $Cu(TMOD)_2$ in supercritical CO_2 is significantly greater than $Cu(TMHD)_2$ [22,23].

Fig. 4 shows the concentration-depth profile of the test stack obtained by XPS analysis. The concentration of copper at the native surface is low due to ambient oxidation and contamination. However, after a few sputtering cycles, the surface layer was removed. In the bulk of the film the atomic ratio of Cu to

O as measured by XPS was not exactly 2 : 1. This is not unexpected and is a consequence of preferential sputtering during Ar^+ depth profiling [24–26]. The apparent composition of Cu_2O after noble gas ion bombardment is reported to be $CuO_{0.36}$ [27], which is in agreement with the stoichiometry observed in our measurements. The interface between Cu_2O and SiO_2 is not well defined due to surface roughness and interdiffusion. We chose to define the Cu_2O/SiO_2 interface as the depth at which the atomic concentration of Cu_2O was equal to that of SiO_2.

Detailed examination of the surface chemistry of the test stack prior to etching is presented in the composite spectra in Fig. 5. The formation of $Cu(OH)_2$ and CuO on the surface of the Cu_2O layer is inevitable upon exposure to ambient conditions. The presence of the Cu^{2+} species within the surface layer is evident when examining the Cu2p signal for the initial sputtering cycles. The shake-up peak located at the higher binding energies of the Cu2p signal is attributed to Cu^{2+}, consistent with the presence of CuO or $Cu(OH)_2$ [28,29]. After 60 s of sputtering, signals from the Cu^{2+} components are no longer detected. The density of Cu_2O is 6.0 g/cm^3, slightly less than that of CuO, 6.00–6.40 g/cm^3. Using the calibrated sputtering rate for Cu_2O (4 nm/min) and neglecting differences in species density, the surface layer containing Cu^{2+} species is determined to be ~4 nm thick. The thickness of the surface layer was also estimated by VASE, which yielded approximate thickness of 5.9 nm with a deviation of 3.2 nm. In terms of thickness, the presence of the surface layer (3–9 nm) is not especially significant relative to the Cu_2O layer (80 nm), however Cu^{2+} species are more resistant to etching with diketones. The surface layer may therefore impact etching of the underlying oxide. We note this effect below.

Etching kinetics were measured using the type B test stack at 100, 125 and 150 °C. To keep the density of the supercritical CO_2 constant at 0.457 g/ml in each of the experiments, the pressures were 19.9, 23.3, and 27.6 MPa at 100, 125 and 150 °C, respectively. The concentration of TMOD in the reactor was 0.02 g/g CO_2. A simple mass balance indicates that this concentration yields more than a 700 fold stoichiometric excess of TMOD relative to the mass of Cu_2O on the wafer sections. After etching, the wafers were analyzed by XPS depth profiling. The sputtering time was converted to thickness using the calibrated sputtering speed of 4 nm/min mentioned above. The results are shown in Fig. 6. After an induction period, the thickness reduction of the Cu_2O layer is nearly linear in time. At 150 °C, the etching rate was 1.49 ± 0.22 nm/min, compared to 0.46 ± 0.17 nm/min at 125 °C and 0.12 ± 0.03 nm/min at 100 °C.

The induction period is most likely due to impurities at the surface and/or the different etching chemistries of cupric and cuprous oxide. George et al. reported that the etching of cupric oxide by Hhfac requires higher temperatures than the etching of cuprous oxide [5]. Their study suggests that cupric oxide must be thermally converted to cuprous oxide prior to etching. To examine the feasibility of direct etching of CuO, we attempted to etch films with thick cupric oxide layers (5 nm) at 125 °C, and 23.0 MPa at a TMOD concentration of 0.02 g/g CO_2. No significant etching was observed even after 4 h. This experiment suggests that cupric oxide formed by ambient exposure serves as a passivation layer that initially inhibits Cu_2O etching.

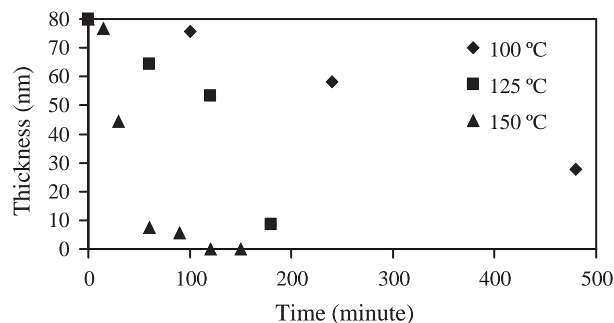

Fig. 6. Remaining Cu_2O layer thickness vs. time for etching with TMOD at 100, 125 and 150 °C at a CO_2 density of 0.457 g/ml. The concentration of TMOD in supercritical CO_2 was 0.02 g/g CO_2. There was induction period at the beginning of each experiment.

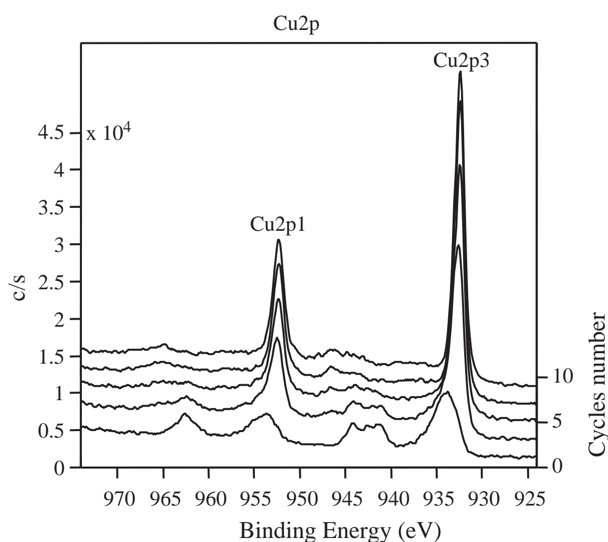

Fig. 5. Composite Cu2p spectra for the first 10 sputtering cycles of a type B test stack prior to etching. Each cycle is represents 30 s of Ar^+ ion sputtering. The Ar^+ ion gun setting was 3 keV, raster size of 2 by 2 mm and 740 nA.

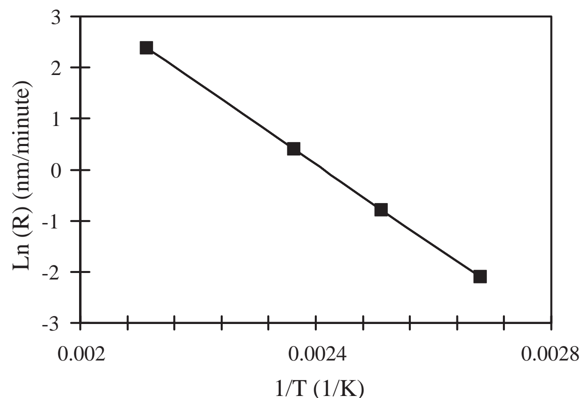

Fig. 7. Cu_2O etching rate vs. temperature for experiments using CO_2 solutions of TMOD in supercritical CO_2 at a TMOD concentration of 0.02 g/g CO_2. The density of CO_2 was 0.457 g/ml.

Assuming Arrehnius kinetics, the activation energy of the etching reaction is calculated to be ~66 kJ/mol (Fig. 7). Although, the thickness of the Cu_2O layer on our test stacks limited the temperature at which we could accurately determine etch rates, it is informative to calibrate etch rates at higher temperatures. At 200 °C, for example, the etch rate is projected to be 10.8 nm/min and an etching time of less than 15 s would be required to remove a 2 nm thick native oxide layer on Cu. A 2 nm thick native copper oxide layer is expected when copper is exposed to air for a short time [30].

4. Conclusion

Etching of cuprous oxide from Cu or SiO_2 substrates in supercritical CO_2 using β-diketone etching agents is effective and efficient. Etching with TMOD at 150 °C proceeds at a rate of 1.5 nm/min with an activation energy of 66 kJ/mol. The formation of Cu^{2+} including CuO and $Cu(OH)_2$ at the surface of Cu_2O during ambient exposure appears to form a passivation layer that initially inhibits CuO etching.

Acknowledgment

Funding from Novellus Systems and The National Science Foundation (CTS 0245002) is gratefully acknowledged. Novellus Systems provided the test wafers used in this study. Instruments supported by the Materials Research Science and Engineering Center at the University of Massachusetts were used in the analysis.

References

[1] C.K. Hu, B. Luther, F.B. Kaufman, J. Hummel, C. Uzoh, D.J. Pearson, Thin Solid Films 262 (1995) 84.
[2] T. Nguyen, L.J. Charneski, D.R. Evans, S.T. Hsu, U.S. Patent No. 5939334, 17 Aug. 1999.
[3] X.Q. Zhao, Y.F. Han, B.X. Liu, J. Appl. Phys 90 (2001) 1638.
[4] J. Farkas, K.M. Chi, M.J. Hampdensmith, T.T. Kodas, L.H. Dubois, Mater. Sci. Eng., B, Solid-State Mater. Adv. Technol. 17 (1993) 93.
[5] M.A. George, D.W. Hess, S.E. Beck, J.C. Ivankovits, D.A. Bohling, A.P. Lane, J. Electrochem. Soc. 142 (1995) 961.
[6] R. Steger, R. Masel, Thin Solid Films 342 (1999) 221.
[7] W. Lee, H.J. Yang, P.J. Reucroft, H.S. Soh, J.H. Kim, S.L. Woo, J. Lee, Thin Solid Films 392 (2001) 122.
[8] W.H. Lee, H.J. Yang, J.Y. Kim, J.G. Lee, C.M. Lee, Y.G. Kim, J. Korean Phys. Soc 40 (2002) 152.
[9] A. Jain, T.T. Kodas, M.J. HampdenSmith, Thin Solid Films 269 (1995) 51.
[10] Y.S. Kim, Y. Shimogaki, J. Vac. Sci. Technol., A, Vac. Surf. Films 19 (2001) 2642.
[11] J.M. Blackburn, D.P. Long, A. Cabanas, J.J. Watkins, Science 294 (2001) 141.
[12] A. Cabanas, D.P. Long, J.J. Watkins, J. Mater. Chem. 16 (2004) 2028.
[13] A. Cabanas, J.M. Blackburn, J.J. Watkins, Microelectron. Eng. 64 (2002) 53.
[14] A. Cabanas, X.Y. Shan, J.J. Watkins, J. Mater. Chem. 15 (2003) 2910.
[15] E. Kondoh, Jpn. J. Appl. Phys., Part 1 43 (2004) 3928.
[16] E.T. Hunde, J.J. Watkins, J. Mater. Chem. 16 (2004) 498.
[17] H. Ohde, S. Kramer, S. Moore, C.M. Wai, J. Mater. Chem. 16 (2004) 4028.
[18] X.R. Ye, C.M. Wai, D.Q. Zhang, Y. Kranov, D.N. McIlroy, Y.H. Lin, M. Engelhard, J. Mater. Chem. 15 (2003) 83.
[19] R.A. Pai, R. Humayun, M.T. Schulberg, A. Sengupta, J.N. Sun, J.J. Watkins, Science 303 (2004) 507.
[20] P.C. Joyce, A. Tipton, K. Shrinivasan, D.W. Hess, S. Myneni, G. Levitin, U.S. Patent No. 6764552, 20 Jul. 2002.
[21] C.A. Bessel, G.M. Denison, J.M. DeSimone, J. DeYoung, S. Gross, C.K. Schauer, P.M. Visintin, J. Am. Chem. Soc. 125 (2003) 4980.
[22] A.F. Lagalante, B.N. Hansen, T.J. Bruno, R.E. Sievers, Inorg. Chem. 34 (1995) 5781.
[23] N.G. Smart, T. Carleson, T. Kast, A.A. Clifford, M.D. Burford, C.M. Wai, Talanta 44 (1997) 137.
[24] J.C. Riviere, in: D. Briggs, M.P. Seah (Eds.), Practical Surface Analysis by Auger and X-ray Photoelectron Spectroscopy, Wiley, Chichester, 1983, p. 34.
[25] G.K. Wehner, in: A.W. Czanderna (Ed.), Methods of Surface Analysis, Methods and Phenomena: Their Applications in Science and Technology, vol. 1, ELSEVIER, Amsterdam, 1975, p. 18.
[26] J.B. Malherbe, S. Hofmann, J.M. Sanz, Appl. Surf. Sci. 27 (1986) 355.
[27] G. Bets, G.K. Wehner, in: R. Behrisch (Ed.), Sputtering by Particle Bombardment II, Topics in Applied Physics, vol. 52, Springer-Verlag, Berlin, 1984, p. 11.
[28] J.F. Watts, An Introduction to Surface Analysis by Electron Spectroscopy, Oxford University Press/Royal Microscopical Society, Oxford, 1990.
[29] J.E. Castle, Surf. Interface Anal. 33 (2002) 196.
[30] S.K. Chawla, B.I. Rickett, N. Sankarraman, J.H. Payer, Corros. Sci 33 (1992) 1617.